Materials Today Physics 46 (2024) 101516

Contents lists available at ScienceDirect

Materials Today Physics

journal homepage: www.journals.elsevier.com/materials-today-physics

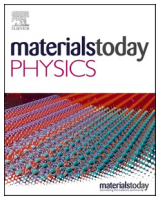

# Generalization of interfacial thermal conductance based on interfacial phonon localization

Ibrahim Al Keyyam , Xinwei Wang *

*Department of Mechanical Engineering, Iowa State University, Ames, IA, 50011, USA*

A R T I C L E I N F O

*Keywords:*
Interfacial thermal conductance
Phonon localization
Equivalent interfacial medium (EIM)
Interface characteristic temperature
Energy carrier transfer time

A B S T R A C T

Interfacial energy transport is of great engineering and scientific importance. Traditional theoretical treatment based on phonon reflection and transmission only provides qualitative understanding of the interfacial thermal conductance ($G$). In the interface region, the material has gradual (covalent) or abrupt (van de Waals) physical structure transition, each transition features interface-region atomic interactions that are different from those of both adjoining sides. This difference makes the interface-region phonons extremely localized. Here, by constructing an "equivalent interfacial medium" (EIM) that accounts for the extremely localized phonon region, $G$ can be described by a universal physical model that is characterized by an "interface characteristic temperature" ($\Theta_{int}$) and energy carrier transfer time. The EIM model fits widely reported $G \sim T$ ($T$: temperature) data with high accuracy and provides remarkable prediction of $G$ at different temperatures based on 2–3 experimental data points. Under normalized temperature ($T/\Theta_{int}$) and interfacial thermal conductance ($G/G_{\max}$), all literature data of $G$ can be universally grouped to a single curve. The EIM model provides a solid correlation between $G$ and interfacial structure and is expected to significantly advance the physical understanding and design of interfacial energy transport toward high-efficiency energy conversion, transport, and micro/nanoelectronics.

## 1. Introduction

As micro/nanoelectronics devices continue to shrink in size and their operational capacities expand, efficient heat dissipation becomes not just a technical challenge but a critical determinant of performance and reliability [1,2]. Therefore, understanding and controlling heat flow at the nanoscale, particularly across interfaces, is vital since interfaces play the pivotal role in dictating overall nanoscale thermal transport [3]. Despite its importance, the mechanisms governing heat dissipation in these microscopic domains are not well understood yet [4,5].

The conventional models of phonon transport at material interfaces, such as the acoustic mismatch model (AMM) [6] and diffuse mismatch model (DMM) [7], have primarily focused on the frequency mismatch between the two materials at the bulk scale and its impact on phonon transmission [8]. These models have great quantitative predictions at low temperatures but lack accuracy when temperature becomes high [9]. The main assumption is that as phonons are incident on the interface, they will either transmit or reflect. The two models treat the interface as a sharp transition from side A to side B, with no transition medium that takes place in between. This of course is not the case for many interfaces where the transition takes place over a finite domain. A great analogy to distinguish both treatments can be drawn from surface chemistry when comparing the Gibbs dividing surface and the Guggenheim interfacial layer [10]. Both models are meant to treat interfacial phenomena in multiphase systems. The former treats the interface as a mathematical dividing plane with zero thickness, while the latter assumes that there exists an interfacial layer of finite thickness best known as the Guggenheim interfacial layer. A more detailed discussion on the relevance of this analogy will be presented in Section 2.

Despite extensive research on interfacial thermal conductance ($G$) measurement [11], a gap persists in seamlessly comparing these measurements across various interfaces. For instance, studies on the interface between diamond and other materials [12] report a wide variance in $G$ values (0.31–128.2 MW $W^{-1}$ $K^{-1}$), highlighting the influence of factors like poor wettability and acoustic mismatch. Moreover, different metal-diamond interfaces [13] exhibit varying sensitivity to temperature variation even when studied under the same temperature range. Hence, developing a cohesive physical framework to model the temperature dependence of $G$ among diverse interfaces aids for a deeper understanding of interfacial thermal transport.

* Corresponding author.
*E-mail address:* xwang3@iastate.edu (X. Wang).

https://doi.org/10.1016/j.mtphys.2024.101516
Received 6 June 2024; Received in revised form 11 July 2024; Accepted 17 July 2024
Available online 18 July 2024

Historically, the Debye model for heat capacity served as a unifying framework for which different solids behave similarly. The key feature for that universality is contained in the characteristic Debye temperature, which encapsulates information about the strength of atomic bonding, the highest frequency the lattice can sustain, and the number of atoms per unit volume. Here, inspired by that universality, we propose a pioneering model to unify the interfacial energy transport across various interfaces by substituting the mathematically thin (zero thickness) interface with a finite-thickness 'equivalent interfacial medium' (EIM). This EIM possesses unique properties that are governed by what we term as the 'interface characteristic temperature' ($\Theta_{int}$). We expect it to be comparable yet distinct from the characteristic Debye temperatures of the adjoining materials for two main reasons. First, the interfacial atomic structure and bonding is different from that of the adjoining materials and hence the thermophysical properties are expected to be different. Second, the physical picture for the EIM is similar to that of disordered solids, where the main energy transport mechanism in the normal direction of the interface is that of localized oscillators of varying sizes and frequencies. As a result, the dominant energy transport is only limited to nearest neighbors, unlike in ordered solids where atoms oscillate collectively to transport energy. This can be understood by the imposed dependency of the oscillators' mean free path on their wavelength as will be elaborated on shortly.

We emphasize that the model proposed here is meant to treat thermal energy transport. The contributions of electrons and phonons exhibit a similarity in the method of analysis that can be well understood through the parallel treatment under the electron/phonon gas models [14]. It becomes, however, more challenging to treat electronic transport across the interface since a discontinuity appears not only in terms of the temperature of the electrons but also in the Fermi level. Electron transport in heterostructures is significantly influenced by the band alignment (conduction and valence bands) at the interface to align the Fermi levels which determines how well electrons can move across it. This alignment results in a unique band structure at the interface, which governs the transport properties of electrons. Despite being fundamentally different, we find this somewhat analogous to what we propose here where the EIM possesses unique properties that differs from the adjoining materials and acts as a bridge to mediate thermal energy. Another substantial difference is that the number of electrons as fundamental particles and electrical charge carriers is conserved unlike phonons which are quasiparticles. This imposes that for charge transport, electrons must physically traverse the interface. Phonons, on the other hand, can get annihilated and created around the interface region and thermal energy can still be mediated without the constraint that phonons must physically go through the interface.

## 2. Physical model development

The physical model for the proposed framework is illustrated in Fig. 1. Instead of a mathematically thin interface, the impact of the interface is substituted with what we term an "equivalent interfacial medium" (EIM) of finite thickness $L$ which better reflects the true underlying physics. As mentioned earlier, this approach is inspired by the Guggenheim interfacial model, where the interface between two separate phases is assumed to be an extended distinct homogenous medium of unique properties that differ from the two phases on each side. The interfacial thermal resistance (ITR) that is usually attributed to the phonon reflections at the interface is now substituted with that of a conduction resistance within the interfacial medium through a distance $L$ as $R'' = L/k$ with $k$ is the equivalent thermal conductivity of the EIM. The reciprocal of the previous expression represents the interfacial thermal conductance defined as $G = k/L$. For covalent-bonded materials, this EIM represents the gradual physical transition that exist between material A and B as depicted in Fig. 1. For an interface between two materials in mechanical contact (e.g., exfoliated 2D material on a substrate), there is a sharp chemical interface from A to B. Therefore, this EIM layer represents the van der Waals force interaction layer between them.

Since the EIM illustrated in Fig. 1 is a mixture of two different materials, and the structure/composition changes from A to B, it is physically reasonable to treat the EIM as an amorphous medium in the normal direction. The structural irregularities, resulting from the formation of an intermixed region, lead to significantly increased phonon scattering. This significantly reduces the phonon mean free path as delineated by several studies in the literature [16]. Turner et al. [17] reported a strong reduction in the phonon lifetime of high entropy alloys FeCoCrMnNi compared with the constituent elements, and is mainly due to the disorder-induced scattering sources associated with the complex disordered unit cell of high entropy alloys. The mass disorder not only promotes phonon-phonon scattering, but is also found to contribute heavily to scattering of low-frequency phonons with electrons as observed by Xu et al. [18] Here, we anticipate similar mechanisms in the interfacial region where the structure is no longer well-defined and regular throughout the EIM. As a result, the interfacial medium is expected to be highly dense with scattering sources and the heat conduction can no longer be treated like in ordered solids.

In crystalline solids, the thermal conductivity varies with temperature due to temperature dependence of heat capacity and phonon population variation, as well as the resulting phonon-phonon scattering change. The thermal conductivity of ordered solids tends to decrease at high temperatures due to Umklapp scattering. Conversely, in amorphous solids, the absence of lattice periodicity complicates phonon dispersion

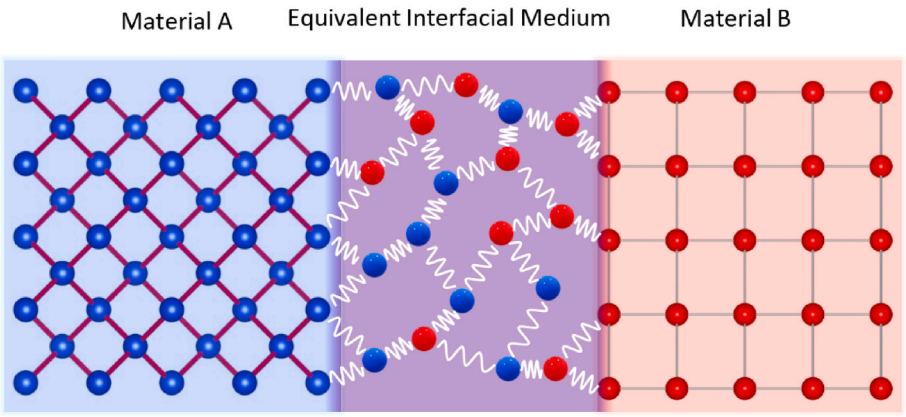


**Fig. 1.** Schematic of the proposed framework. The EIM has distinct properties different from those of Material A and B. The interfacial medium has a continuous change of physical structure from A to B, a very strong mass disorder in the thickness direction, and can be regarded amorphous in this direction. The schematic is partially made by VESTA software [15].

and challenges the well-established thermal transport models of crystalline solids [19]. The thermal conductivity of amorphous solids shows a monotonic increase with temperature, which becomes very minute and almost saturates at high temperatures. In 1911, Einstein [20] proposed a model for the thermal conductivity by assuming that atoms vibrate independently with a single frequency and uncorrelated phase, and heat conduction follows a random walk of these oscillators, coupled to the three nearest neighbors. This model failed to capture the magnitude and even to dictate the temperature dependency for crystalline materials. However, it has been found to be very relevant for amorphous solids and has been developed further by Cahill. et al. [21] to predict the minimum thermal conductivity of disordered materials. In Cahill's formulation, the modifications included large entity oscillators with mean free paths as half of their wavelengths and linear dispersion as in the low-frequency acoustic waves in the Debye model. Despite introducing large oscillating entities, their model maintained the random walk picture as the dominant mechanism for energy transport.

While Cahill's model is meant to describe the minimum thermal conductivity of amorphous solids, we find the assumption of a mean free path equal to half the wavelength of the oscillator is remarkably consistent with the picture of the interfacial structure. There is no wave that can sustain more than a half oscillation across the interface before it loses its identity. This is simply because in the interfacial medium, the physical structure keeps changing from A to B. The thermal conductivity under this formulation is defined as in Equation (1):

$$\kappa = \left(\frac{\pi}{6}\right)^{1/3} k_B n^{2/3} \sum_i v_i \left(\frac{T}{\Theta_{int}}\right)^2 \int_0^{\Theta_{int}/T} \frac{x^3 e^x}{(e^x-1)^2} dx \quad (1)$$

here, $k_B$ is the Boltzmann constant, $n$ the number of atoms per unit volume and is taken to be the harmonic average of the adjoining materials that constitute the interface, $\Theta_{int}$ is what we term as the interface characteristic temperature which encapsulates the unique properties of the EIM and is defined as $\Theta_{int} = v_{avg.int}(\hbar/k_B)(6\pi^2 n)^{1/3}$. We emphasize that the choice for taking the harmonic average for $n$ will only impact the interaction time ($\tau$, defined below) but will not impact $\Theta_{int}$ at all. We relax the conditions and assume that the group velocity of the oscillators is independent from their polarization and hence the sum can be reduced as $\sum_i v_i = 3v_{avg.int}$, where $i$ is the index to sum over the three polarizations. This is a well-adopted approximation for the Debye model that will tremendously simplify the computations. We then combine $v_{avg.int}$ and $L$ into a single parameter termed as the energy carrier transfer time defined as $\tau = L/v_{avg.int}$, which is the time taken for the energy carrier to transfer through the EIM. The final expression of $G$ is then defined as follows:

$$G = \frac{3}{\tau}\left(\frac{\pi}{6}\right)^{1/3} k_B n^{2/3} \left(\frac{T}{\Theta_{\mathrm{int}}}\right)^2 \int_0^{\Theta_{int}/T} \frac{x^3 e^x}{(e^x-1)^2} dx \quad (2)$$

## 3. Results and discussion

### 3.1. Interface characteristic temperature and energy transfer time

As depicted in Fig. 2, we prove that various interfaces can be fitted very accurately to our proposed model. Several other interfaces are fitted and summarized in Table 2. Previous studies have suggested that the temperature dependency of $G$ follows the same one as the lower Debye temperature material of the adjoining materials [22]. The physics behind such assumption is that at low temperatures, well below the Debye temperatures of both materials, $G$ increases with increased temperature since more phonon modes become populated as temperature rises, allowing more channels for heat transfer across the interface. As the temperature approaches the Debye temperature of one of the materials (say material A), $G$ tends to saturate. This is because all the phonon modes in material A are already excited, so further increase in temperature cannot significantly increase the phonon population in material A that can transport heat across the interface. While the

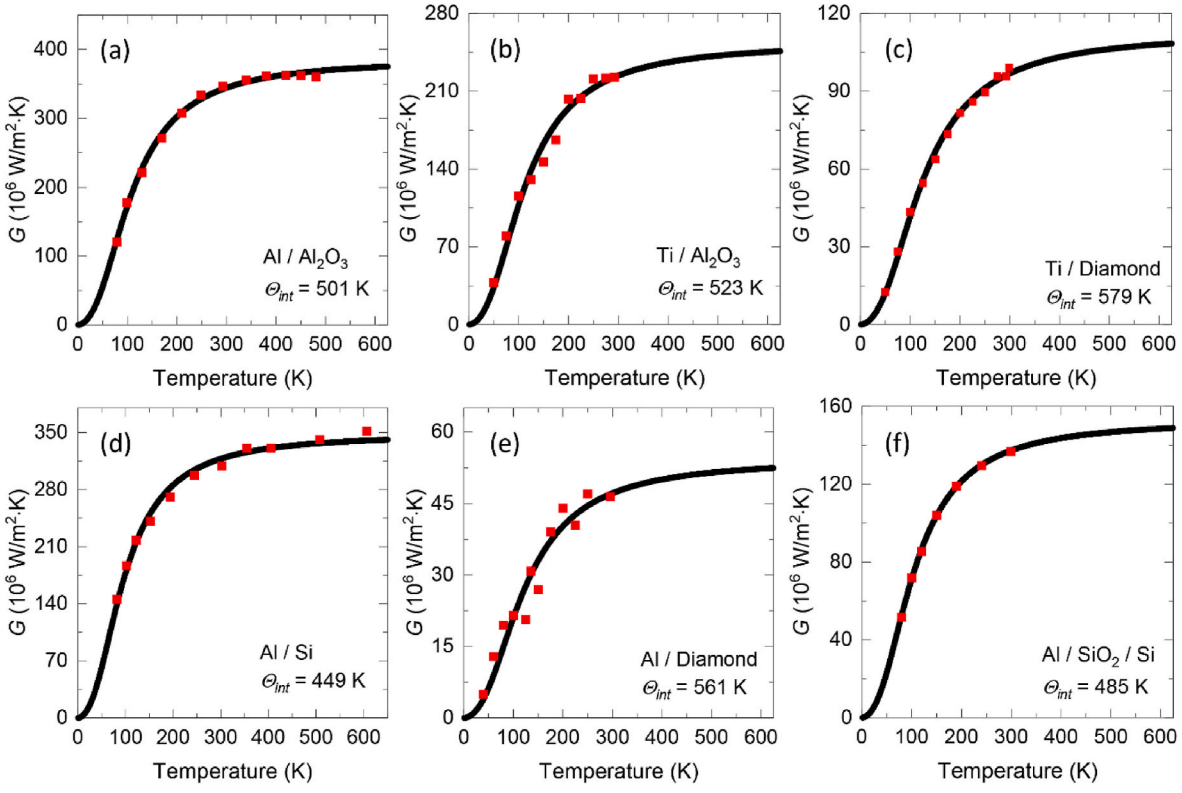


**Fig. 2.** The experimental data of the interfacial thermal conductance ($G$) fitted to our proposed model for (a) Al/$Al_2O_3$ (b) Ti/$Al_2O_3$ (c) Ti/Diamond (d) Al/Si (e) Al/Diamond (f) Al/$SiO_2$/Si. The interface characteristic temperature ($\Theta_{int}$) is shown for each interface.

**Table 1**
The Debye temperature, the longitudinal acoustic ($v_{LA}$), transverse acoustic ($v_{TA}$), and average ($v_{avg}$) phonon group velocity of the materials that constitute the interfaces considered in this study.

| Material | Debye Temperature (K) | $v_{LA}$ (m/s) | $v_{TA}$ (m/s) | $v_{avg}$ (m/s) |
|---|---|---|---|---|
| Al | 433 [23] | 6240 [7] | 3040 [7] | 3520 |
| $Al_2O_3$ | 980 [28] | 10890 [7] | 6450 [7] | 7286 |
| Au | 165 [23] | 3390 [7] | 1290 [7] | 1526 |
| Cu | 343 [23] | 4910 [7] | 2500 [7] | 2881 |
| Diamond | 2230 [23] | 17500 [7] | 12800 [7] | 13925 |
| GaN | 600 [29] | 7885 [30] | 4140 [30] | 4753 |
| $MoS_2$ | 210 [26] | 6500 [31] | 4400 [31] | 4861 |
| Si | 645 [23] | 8970 [7] | 5332 [7] | 6020 |
| $SiO_2$ | 470 [27] | 6090 [7] | 4100 [7] | 4534 |
| Ti | 420 [23] | 6070 [7] | 3125 [7] | 3596 |
| ZnO | 400 [28] | 6090 [30] | 2760 [30] | 3219 |

**Table 2**
A summary for interface characteristic temperature ($\Theta_{int}$), the upper limit of $G$ ($G_{max}$), normalized $G$ at room temperature $\gamma = G_{RT}/G_{max}$, interaction time ($\tau$), the average group velocity of the carriers in the EIM ($v_{avg,int}$), and the thickness of the EIM ($L$) for studied interfaces.

| Interface (A/B) | $\Theta_{int}$ (K) | $G_{max}$ (MW/m$^2$•K) | $\gamma$ at 298 K | $\tau$ (ps) | $v_{avg.int}$ (m/s) | $L$ (nm) |
|---|---|---|---|---|---|---|
| Al/$SiO_2$ [35] | 204 | 42.1 | 99.7 % | 4.79 | 1952 | 9.35 |
| Au/Diamond [13] | 427 | 41.4 | 93.7 % | 6.53 | 3545 | 23.2 |
| Al/Si [36] | 432 | 373 | 93.5 % | 0.633 | 3822 | 2.42 |
| Al/Si [32] | 449 | 342 | 92.9 % | 0.692 | 3972 | 2.75 |
| Al/$SiO_2$/Si [32] | 485 | 150 | 91.3 % | 1.35 | 4641 | 6.27 |
| Al/$Al_2O_3$ [33] | 501 | 378 | 90.9 % | 0.550 | 4722 | 2.6 |
| Ti/$Al_2O_3$ [13] | 523 | 248 | 90.0 % | 0.758 | 5183 | 3.93 |
| Al/$Al_2O_3$ [13] | 536 | 193 | 89.5 % | 1.08 | 5052 | 5.46 |
| Al/Diamond [13] | 561 | 53.2 | 88.4 % | 7.10 | 3927 | 27.9 |
| Ti/Diamond [13] | 579 | 110 | 87.7 % | 3.69 | 3903 | 14.4 |
| ZnO/GaN [37] | 620 | 544 | 85.9 % | 0.362 | 6010 | 2.18 |
| Cu/$Al_2O_3$ [25] | 901 | 332 | 72.4 % | 0.598 | 8695 | 5.2 |
| Cu/Al [25] | 1213 | 6435 | 56.4 % | 0.0416 | 10083 | 0.42 |
| $MoS_2$/$SiO_2$ [22] | 1460 | 28.6 | 46.9 % | 4.76 | 17008 | 81 |

previous claim is qualitatively true it is not very accurate as per the extracted results for the $\Theta_{int}$.

For interfaces of covalent bonding and most interfaces, we find that $\Theta_{int}$ takes an intermediate value between the Debye temperatures of the two materials forming the interface but indeed is more comparable to the lower Debye temperature. The discrepancy between $\Theta_{int}$ and the lower Debye temperature of the adjoining materials becomes more prominent when a large mismatch in the Debye temperatures exists between the two materials that form the interface. We interpret this as the following. At temperatures above the lower Debye temperature of material A, if the Debye temperature of the other material (material B) is significantly higher, $G$ can continue increasing with temperature due to the large accessible high-frequency phonon modes in material B that can scatter inelastically via anharmonic interactions to contribute to the thermal transport across the interface. This is particularly prominent for metal-Diamond interfaces where there is a large mismatch in the Debye temperature. For instance, the Debye temperature of Au and Diamond are 165 and 2230 K, respectively [23], whereas the $\Theta_{int}$ for Au/Diamond is found to be 427 K which is 2–3 times higher than for Au. It has been observed experimentally that $G$ for metal/Diamond interfaces is almost 1–2 orders of magnitude larger than predicted using the acoustic mismatch model [24]. This enhancement in $G$ for acoustically mismatched interfaces is partially explained by inelastic scattering contribution at the interface, especially at high temperatures where the anharmonicity causes a redistribution of the spectral flux of the excited phonons during their propagation and thus facilitates energy transfer between phonons of different frequencies. Electron-phonon interactions in the metal film could also contribute to thermal transport at metal/-nonmetal interface as will be discussed in Section 3.4.

Some anomalous observations are observed for Cu/Al and $MoS_2$/$SiO_2$ interfaces where the extracted $\Theta_{int}$ exceed the Debye temperatures of the forming materials. The former is a metallic interface and the discrepancies between the reported Debye temperature for Al and Cu (428 and 343 K, respectively) [23] and the inferred $\Theta_{int}$ (1213 K) can be directly attributed to the large enhancement in heat transport due to electronic contribution which dominates the heat conduction as delineated in the published work of Gundrum et al. [25]. We speculate that the latter situation ($MoS_2$/$SiO_2$) is mainly because the interface phonons are sustained by van der Waals bonding while those of $MoS_2$ (in-plane phonons) and $SiO_2$ are sustained by covalent bonding. The reported Debye temperatures for those phonons are 262 K for a monolayer $MoS_2$ [26] and 470 K for $SiO_2$ [27] as shown in Table 1. We do not expect the interface characteristic temperature to be comparable to those Debye temperatures since they are sustained by different atomic bonding. Overall, we believe that $\Theta_{int}$ can serve as a reliable metric to dictate the temperature dependency and can hint to non-phononic heat conduction when the inferred $\Theta_{int}$ is significantly larger than the Debye temperatures of the adjoining materials.

As mentioned earlier, $\Theta_{int}$ is related to $v_{avg.int}$ through the same definition for the characteristic Debye temperature. While the physical picture is completely different in our model than in ordered solids, the magnitude of $v_{avg.int}$ calculated from $v_{avg.int} = \Theta_{int}\,(k_B/\hbar)\left(6\pi^2 n\right)^{-1/3}$ is of the order $10^3$–$10^4$ m/s as summarized in Table 2. The energy carrier transfer time ($\tau$), presented in Tables 2, is observed to be roughly of the order 0.1–1 ps (ps). The order of magnitude of the interfacial region thickness ($L$) can then be estimated from $L = v_{avg.int}\tau$ to be of the order 1–10's nm, which is of the order of the actual thickness of typical interfacial regions observed experimentally [32–34]. The EIM thickness is calculated for various interfaces and summarized in Table 2. Interestingly, we observe that metal-Diamond interfaces are of the order $10^{-8}$ m which is one order of magnitude larger than the rest of interfaces, except for $MoS_2$/$SiO_2$ which had the largest thickness estimated as 81 nm. A plausible reason for such thicker EIM is due to the lattice-mismatched nature of metal/diamond interface due to the small lattice constant of diamond. It is generally known that smaller mismatches allow for better growth and stronger interfaces, while larger mismatches can lead to defects, strain, and potential delamination issues. This thicker EIM is expected to induce a larger interfacial thermal resistance which goes hand in hand with the lower predicted $G_{\max}$ particularly for Au/Diamond and Al/Diamond. On the other hand, $\tau$ for Cu/Al interface found to be the shortest with 0.0416 ps. We interpret this abnormal short time by the electronic domination over the heat conduction in metals which adds additional superior channels to mediate heat at the interface and hence reduce the time it takes for the energy to get mediated. The carrier velocity $v_{avg.int}$ for this interface is found to be ~10 km/s that is roughly 3–4 times larger than the phonon group velocity for Cu–Al, respectively. This ensures that there exists another channel (electrons contribution) for which the heat is mediated across the Cu/Al interface.

Generally, we find that $v_{avg.int}$ takes an intermediate value between the sound speed of materials that form the interface. Considering that the EIM is a mixture of the two materials, this goes in hand with the sound velocity in alloys which depends linearly on the alloying concentration and is bound between the sound speeds of the two materials that form the alloy. For instance, for Al/Si interface, the sound velocity is

expected to be in the range 3520 and 6020 m/s (see Table 1) which represent the average sound speed in Al and Si, respectively. We find the extracted values of $v_{avg.int}$ for Al/Si interface to be quantitatively consistent with the above argument. It is calculated to be 3822 and 3972 m/s as shown in Table 2. This makes the EIM region seem to be more dominated by the material with the lower sound velocity (aluminum for Al/Si interface).

### 3.2. Upper limit of interfacial thermal conductance ($G_{max}$)

It is well reported in literature that $G$ saturates and reaches a plateau at high temperatures for most interfaces. While this can be qualitatively understood by the saturation of the heat capacity at around the lower Debye temperature of the two materials, a quantitative prediction of the saturation temperature for $G$ remains untouched. Using this model, one can predict the temperature at which the interfacial energy transport, characterized by $G$, becomes insensitive to the change of environmental temperature. This could be crucial for certain applications where precise thermal management is needed. We demonstrate that this temperature range could substantially exceed the lower Debye temperature of the adjoining materials, unlike the prenotion for most well-adopted theories. Moreover, the model provides a quantitative prediction for the maximum $G$ termed as the interfacial conductance upper limit: $G_{max}$. In Fig. 3, we demonstrate this by making use of only three data points for measured $G$ at low temperatures (marked as blue solid triangles) as inputs to our model, the predicted $G_{max}$ where the blue line saturates, is in great agreement with the reported data. Several methods attempted in literature to enhance $G$ [38–40]. Therefore, it is of interest to have an intuition about the maximum $G$ an interface can sustain prior to implementing further enhancements. The relation of $G$ relative to the $G_{max}$ is encapsulated in the normalized interfacial thermal conductance ($\gamma$) defined as $\gamma = G/G_{max}$. Table 2 provides calculated values of $\gamma$ at room temperature (RT) for the various interfaces found in literature. It is found quite many interfaces' $G$ at RT is close to $G_{max}$, and there is little room to further improve by increasing temperature.

### 3.3. Facilitating experimental characterization

The experimental techniques used to measure the temperature dependence of $G$ are quite exhaustive, where the experiment must be repeated several times at different temperatures. The difficulties are magnified when conducting experiments at cryogenic temperatures, where special apparatus and precise cooling techniques are necessary to maintain the accuracy. Here, we demonstrate that dictating the temperature-dependency $G$ can be accurately achieved with as few as three careful measurements at around room temperature as demonstrated in Fig. 3 (data points used are marked as red solid squares). This approach drastically reduces the experimental effort while maintaining a prediction accuracy within less than a 10 % error margin as shown in Fig. 3c–e. This margin is within the accepted experimental uncertainty for any measurement technique.

The temperature dependence of Debye temperature is a well-established concept that has been confirmed experimentally in literature [41]. While this work is not mainly concerned with investigating if such dependency applies for $\Theta_{int}$, a similar observation is made where the $\Theta_{int}$ at low temperatures (shown in blue) and those at high temperatures (shown in red) in Fig. 3 are somewhat different. Such discrepancies are partially due to the variation of $\Theta_{int}$ with temperature (interface structure changes with temperature) as well as due to experimental uncertainties. Although the results shown in Fig. 3 are relying

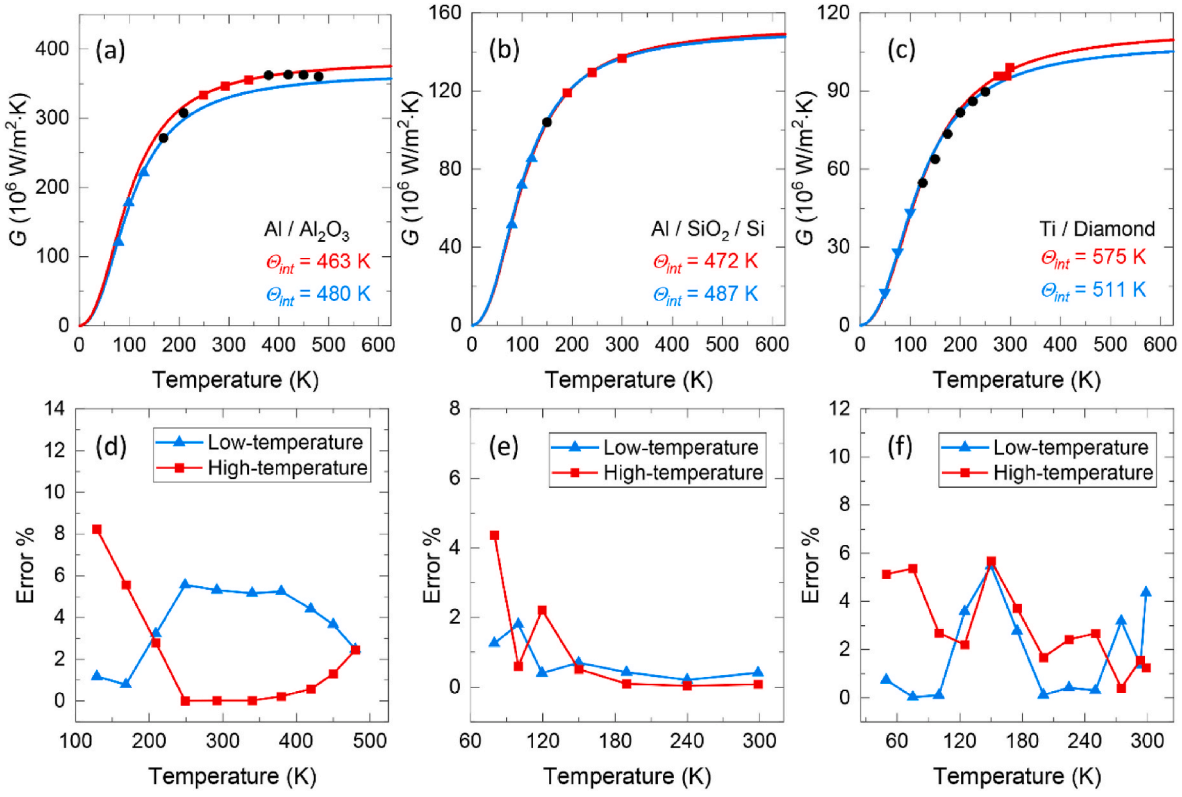


**Fig. 3.** The prediction for $G$ using three data points at low (blue) and room (red) temperatures as inputs to our model for (a) Al/$Al_2O_3$. (b) Al/$SiO_2$/Si. (c) Ti/Diamond. For low-temperature measurements (blue line), the predicted $G_{max}$ is in great agreement with the experimental reported values. For room-temperature measurements (red line), we show that three measurements suffice for dictating the temperature dependency of $G$ across the entire temperature range. We emphasize that only data points with matching color as the lines are used to generate the prediction, while the rest of the data points are just mapped on the graph. The relative error of the prediction compared with experimental data is shown for (d) Al/$Al_2O_3$, (e) Al/$SiO_2$/Si, and (f) Ti/Diamond. (For interpretation of the references to color in this figure legend, the reader is referred to the Web version of this article.)

on 3 data points, we have demonstrated that using two data points with sufficient variation in $G$ between them also yields a remarkable accurate prediction as shown in Fig. S1 of the Supplementary Material which serves as a guide on how to use the model. We further test the sensitivity of the prediction to the choice of the data points for $Al/Al_2O_3$ interface taken as a case study. The results are illustrated in Fig. S2 where the prediction remained within the claimed uncertainty, which ensures the versatility of the proposed work.

We further examine our proposed $\Theta_{int}$ and $G_{max}$ concepts by attempting to normalize the reported $G$ in literature to $G_{max}$ for various interfaces aiming to produce one universal plot for all data reported in the literature. This attempt is inspired by the work of Peter Debye on the heat capacity of solids, where different materials show a universal temperature dependence when normalized to their Debye temperatures. The key difference is that $G_{\max}$ is unique for each interface, while the molar heat capacity for solids converges to the classical prediction by the Dulong-Petit law. Very strikingly, the results exhibit a universality analogous to the sought one as shown in Fig. 4b despite the significant scattered data shown in Fig. 4a. The results demonstrate that $G$ for various interfaces, regardless of their type of bonding, follow the same temperature dependency when normalized against their $\Theta_{int}$.

The interfacial thermal resistance is conventionally attributed to energy carrier (phonons and/or electrons) reflection at the interface, which arises due to several reasons. The most obvious one is due to the change in the medium when transmitting from side A to side B. Even when both sides are of the same material, if the transition happens through different crystallographic orientation, it will induce a thermal resistance as well due to structural disorder. This structural disorder which takes place spatially over a finite thickness can also be well-modeled by the proposed work. Moreover, for exfoliated 2D materials such as in $MoS_2/SiO_2$ [22] interfaces, the contact is usually sustained via mechanical means. Even though atomic-layer exfoliated materials have minimal defects and the transition from side A to side B is atomically sharp, the interactions between atoms of side A and side B in the direction normal to the interface sustained via the weak van der Waals (vdW) force. This interaction takes place over a finite region that is equivalent to what we refer to as the EIM and induces a thermal resistance that can be well-captured by the current work.

### 3.4. Limitations of the current study and future outlook

Phonons, the main heat carriers in non-metallic materials, are conventionally understood to traverse elastically across the interface. Notable exceptions occur when the interfacing materials exhibit substantial mismatch in their Debye temperatures. Nonetheless, recent investigations have revealed that interfaces between materials with similar Debye temperatures may also facilitate a considerable measure of inelastic phonon transmission, particularly at high temperatures. The inelastic phonon transmission adds another channel to mediate the heat which yields further enhancement of the thermal conductance at the interface. This phenomenon has been reported by Li. et al. [32], where the Al/GaN interface shows a pronounced linear increase in $G$ in the high-temperature range of 500–800 °C, which can somewhat also be observed in Fig. 2d for the Al/Si interface. We emphasize that our model is not based on phonon transmission across the interface. Rather it interprets the interfacial $G$ by extremely localized phonon transport within the EIM, which makes the model itself strongly relies on the structure of the EIM. Despite the completely different proposition here, we find it can still accurately fit the $G$ data that is originally explained by enhanced inelastic phonon transmission.

Moreover, electron-phonon coupling at metal/non-metal interfaces critically affects thermal and electrical transport in thin films and heterostructures since it dictates the rate of energy dissipation and electron cooling, especially under nonequilibrium conditions. Studies on gold films [42] and heterostructures [43] demonstrate that the substrate's thermal properties and film thickness significantly influence electron-phonon coupling which contribute to the overall thermal transport. Even though the current work can capture the temperature-dependency of $G$ for metallic/non-metallic interfaces as shown in Fig. 2, the distinct contribution of electrons and phonons cannot be distinguished in the current state of the model. We speculate that this contribution has been reflected as a larger $\Theta_{int}$ compared to the lower Debye temperature of the adjoining materials. An exception is the $Al/SiO_2$ interface reported by Ref. [35] where the $\Theta_{int}$ (204 K) is observed to be lower than the Debye temperatures of both Al and Si (433 and 645 K, respectively) shown in Table 2. Our model has been formulated as if thermal transport is mediated via the localized oscillators within the EIM. We anticipate that the assumption that electrons and phonons in the metal side are in thermal equilibrium breaks down around the EIM since phonons in the metals are strongly coupled to those in the substrate via the localized phonons in the EIM. This creates an additional channel to mediate the heat through electron-phonon interactions in the metallic film but is not disentangled in the current model. Future efforts could be devoted to incorporating more of the detailed physics for such complex transport processes. However, our results suggest that the prediction of $G$ seems to be insensitive to the detailed mechanisms by which the heat is sustained in the vicinity of the EIM and the assumption that the heat is mainly carried via the localized phonons within the EIM seems to suffice for an accurate prediction.

We emphasize that this work, as reported here, cannot yet serve as a

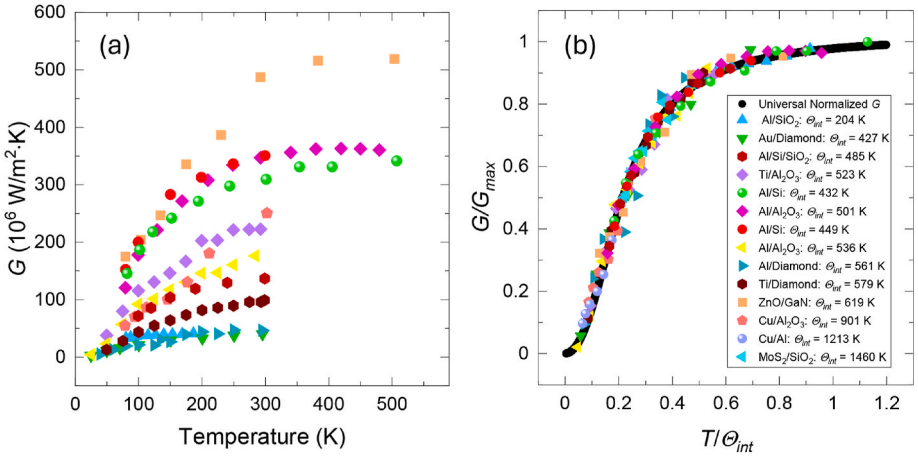


**Fig. 4.** The reported $G$ for various interfaces. (a) As reported in literature. Note: Cu/Al is excluded for its large order of magnitude ~ GW. (b) Normalized to their predicted $G_{\max}$ while the temperature scale is normalized to the proposed $\Theta_{int}$. The results resemble the universal temperature dependency of heat capacity of solids when normalized to their Debye temperatures.

standalone model to predict the variation of $G$, where it must be aided with minimal experimental work. The proposed study marks the cornerstone to explore the interfacial thermal conductance from a fresh perspective and we note that several questions are yet to be investigated. The most obvious and crucial one is: Can we, by any means, estimate the unique properties of the equivalent interfacial medium which are encapsulated mainly in $\Theta_{int}$ without the reliance on experimental data? Future efforts will be dedicated to investigating this.

## 4. Conclusion

We developed a pioneering model to shed new lights on the physics of the interfacial thermal conductance ($G$) for various interfaces reported in literature. The proposed equivalent interfacial medium (EIM) model accounts for the localized phonons in the interface-regionwhich sustain the interfacial heat conduction. The work yields a universal temperature dependency analogous to that of heat capacity of solids under the Debye model. The EIM model was found to greatly fit all the literature data for $G$ variation with temperature. The localized phonons feature two key parameters: interface characteristic temperature ($\Theta_{int}$) and energy transfer time, whose physics can be well interpolated by the atomic bonding strength, phonon velocity, and equivalent interface medium thickness. Under normalized temperature ($T/\Theta_{int}$) and interfacial thermal conductance ($G/G_{max}$), all literature data can be universally grouped together to a single curve. We demonstrate that one can conduct 2–3 measurements for $G$ and get a remarkably accurate prediction for it at any temperature of interest within the uncertainty of any experimental technique. We expect the EIM model will attract broad interests for scientific understanding and engineering design of interfaces for material design, process control, and micro/nanoelectronics development.

## CRediT authorship contribution statement

**Ibrahim Al Keyyam:** Writing – original draft, Methodology, Investigation, Formal analysis, Data curation, Conceptualization. **Xinwei Wang:** Writing – review & editing, Supervision, Project administration, Methodology, Investigation, Funding acquisition, Formal analysis, Data curation, Conceptualization.

## Declaration of competing interest

The authors declare the following financial interests/personal relationships which may be considered as potential competing interests: Xinwei Wang reports financial support was provided by National Science Foundation. If there are other authors, they declare that they have no known competing financial interests or personal relationships that could have appeared to influence the work reported in this paper.

## Data availability

Data will be made available on request.

## Acknowledgement

Partial support of this work by the US National Science Foundation (CMMI2032464) is gratefully acknowledged.

## Appendix A. Supplementary data

Supplementary data to this article can be found online at https://doi.org/10.1016/j.mtphys.2024.101516.

## References

[1] B. Yang, J. Wang, Z. Yang, Z. Xin, N. Zhang, H. Zheng, X. Wu, Thermal transport mechanism of AlN/SiG/3C–SiC typical heterostructures, Mater. Today Phys. 30 (2023): 100948.
[2] E. Pop, Energy dissipation and transport in nanoscale devices, Nano Res. 3 (3) (2010) 147–169.
[3] J. Pan, X. Fan, K. Zhang, Z. Geng, J. Yao, Y. Deng, J. Zhou, X.-J. Yan, M.-H. Lu, H. Lu, Y.-F. Chen, Effective interface engineering for phonon manipulation in an Al/ErAs/GaAs system, Mater. Today Phys. 28 (2022): 100897.
[4] Y.-J. Wu, T. Zhan, Z. Hou, L. Fang, Y. Xu, Physical and chemical descriptors for predicting interfacial thermal resistance, Sci. Data 7 (1) (2020) 36.
[5] I. Al Keyyam, M. Rahbar, E. Shi, B. Li, T. Wang, X. Wang, Thermal conductance between <6 nm single-walled carbon nanotube bundle and Si substrate, J. Phys. Chem. C (2024) 1505–1517.
[6] W.A. Little, The transport of heat between dissimilar solids at low temperatures, Can. J. Phys. 37 (3) (1959) 334–349.
[7] E.T. Swartz, R.O. Pohl, Thermal boundary resistance, Rev. Mod. Phys. 61 (3) (1989) 605–668.
[8] X. Li, J. Han, S. Lee, Thermal resistance from non-equilibrium phonons at Si–Ge interface, Mater. Today Phys. 34 (2023): 101063.
[9] I. Al Keyyam, M. Rahbar, N. Hunter, B. Li, T. Wang, E. Shi, X. Wang, $T^{-n}$ ($n$: 2.4~2.56) temperature dependence of thermal resistance at single-walled carbon nanotubes/$SiO_2$ interface at <8 nm scale, Int. J. Heat Mass Tran. 226 (2024): 125513.
[10] E.A. Guggenheim, N.K. Adam, F.G. Donnan, The thermodynamics of adsorption at the surface of solutions, Proc. Roy. Soc. Lond. A 139 (837) (1933) 218–236.
[11] J. Liu, I. Al Keyyam, Y. Xie, X. Wang, Perspectives on interfacial thermal resistance of 2D materials: Raman characterization and underlying physics, Surf. Sci. Technol. 2 (1) (2024) 8.
[12] Z. Cheng, F. Mu, L. Yates, T. Suga, S. Graham, Interfacial thermal conductance across room-temperature-bonded GaN/diamond interfaces for GaN-on-Diamond devices, Appl. Mater. Interfaces 12 (7) (2020) 8376–8384.
[13] R.J. Stoner, H.J. Maris, Kapitza conductance and heat flow between solids at temperatures from 50 to 300 K, Phys. Rev. B 48 (22) (1993) 16373–16387.
[14] G. Chen, Nanoscale energy transport and conversion: a parallel treatment of electrons, in: Molecules, Phonons, and Photons, Oxford Univ. Press, 2005.
[15] K. Momma, F. Izumi, VESTA 3 for three-dimensional visualization of crystal, volumetric and morphology data, J. Appl. Crystallogr. 44 (6) (2011) 1272–1276.
[16] K. Kothari, M. Maldovan, Phonon surface scattering and thermal energy distribution in superlattices, Sci. Rep. 7 (1) (2017) 5625.
[17] S.R. Turner, S. Pailhès, F. Bourdarot, J. Ollivier, Y. Sidis, J.-P. Castellan, J.-M. Zanotti, Q. Berrod, F. Porcher, A. Bosak, M. Feuerbacher, H. Schober, M. De Boissieu, V.M. Giordano, Phonon behavior in a random solid solution: a lattice dynamics study on the high-entropy alloy FeCoCrMnNi, Nat. Commun. 13 (1) (2022) 7509.
[18] Q. Xu, J. Zhou, T.-H. Liu, G. Chen, Effect of electron-phonon interaction on lattice thermal conductivity of SiGe alloys, Appl. Phys. Lett. 115 (2) (2019): 023903.
[19] P. Sheng, M. Zhou, Heat conductivity of amorphous solids: simulation results on model structures, Science 253 (5019) (1991) 539–542.
[20] A. Einstein, Elementare Betrachtungen über die thermische Molekularbewegung in festen Körpern, Ann. Phys. 340 (9) (1911) 679–694.
[21] D.G. Cahill, S.K. Watson, R.O. Pohl, Lower limit to the thermal conductivity of disordered crystals, Phys. Rev. B 46 (10) (1992) 6131–6140.
[22] E. Yalon, B. Aslan, K.K.H. Smithe, C.J. McClellan, S.V. Suryavanshi, F. Xiong, A. Sood, C.M. Neumann, X. Xu, K.E. Goodson, T.F. Heinz, E. Pop, Temperature-dependent thermal boundary conductance of monolayer $MoS_2$ by Raman thermometry, ACS Appl. Mater. Interfaces 9 (49) (2017) 43013–43020.
[23] C. Kittel, Introduction to Solid State Physics, 8 ed., Wiley, 2004.
[24] W. Miao, M. Wang, Importance of electron-phonon coupling in thermal transport in metal/semiconductor multilayer films, Int. J. Heat Mass Tran. 200 (2023): 123538.
[25] B.C. Gundrum, D.G. Cahill, R.S. Averback, Thermal conductance of metal-metal interfaces, Phys. Rev. B 72 (24) (2005): 245426.
[26] S.V. Suryavanshi, A.J. Gabourie, A.B. Farimani, E. Yalon, E. Pop, Thermal boundary conductance of the $MOS_2$-$SiO_2$ interface, in: IEEE 17th Int. Conf. Nanotechnol., 2017, pp. 26–29, 2017.
[27] W. Zhu, G. Zheng, S. Cao, H. He, Thermal conductivity of amorphous $SiO_2$ thin film: a molecular dynamics study, Sci. Rep. 8 (1) (2018): 10537.
[28] J.A. Spencer, A.L. Mock, A.G. Jacobs, M. Schubert, Y. Zhang, M.J. Tadjer, A review of band structure and material properties of transparent conducting and semiconducting oxides: $Ga_2O_3$, $Al_2O_3$, $In_2O_3$, ZnO, $SnO_2$, CdO, NiO, CuO, and $Sc_2O_3$, Appl. Phys. Rev. 9 (1) (2022): 011315.
[29] C. Roder, S. Einfeldt, S. Figge, D. Hommel, Temperature dependence of the thermal expansion of GaN, Phys. Rev. B 72 (8) (2005): 085218.
[30] X. Wu, J. Lee, V. Varshney, J.L. Wohlwend, A.K. Roy, T. Luo, Thermal conductivity of wurtzite zinc-oxide from first-principles lattice dynamics – a comparative study with gallium nitride, Sci. Rep. 6 (1) (2016): 22504.
[31] K. Kaasbjerg, K.S. Thygesen, K.W. Jacobsen, Phonon-limited mobility in $n$-type single-layer $MoS_2$ from first principles, Phys. Rev. B 85 (11) (2012): 115317.
[32] Q. Li, F. Liu, S. Hu, H. Song, S. Yang, H. Jiang, T. Wang, Y.K. Koh, C. Zhao, F. Kang, J. Wu, X. Gu, B. Sun, X. Wang, Inelastic phonon transport across atomically sharp metal/semiconductor interfaces, Nat. Commun. 13 (1) (2022) 4901.
[33] Z. Cheng, Y.R. Koh, H. Ahmad, R. Hu, J. Shi, M.E. Liao, Y. Wang, T. Bai, R. Li, E. Lee, E.A. Clinton, C.M. Matthews, Z. Engel, L. Yates, T. Luo, M.S. Goorsky, W. A. Doolittle, Z. Tian, P.E. Hopkins, S. Graham, Thermal conductance across

harmonic-matched epitaxial Al-sapphire heterointerfaces, Commun. Phys. 3 (1) (2020) 115.
[34] D. Xu, R. Hanus, Y. Xiao, S. Wang, G.J. Snyder, Q. Hao, Thermal boundary resistance correlated with strain energy in individual Si film-wafer twist boundaries, Mater. Today Phys. 6 (2018) 53–59.
[35] D. Cahill, A. Bullen, S.-M. Lee, Interface thermal conductance and the thermal conductivity of multilayer thin films, High. Temp. - High. Press. 32 (2) (2000) 135–142.
[36] A.J. Minnich, J.A. Johnson, A.J. Schmidt, K. Esfarjani, M.S. Dresselhaus, K. A. Nelson, G. Chen, Thermal conductivity spectroscopy technique to measure phonon mean free paths, Phys. Rev. Lett. 107 (9) (2011): 095901.
[37] J.T. Gaskins, G. Kotsonis, A. Giri, S. Ju, A. Rohskopf, Y. Wang, T. Bai, E. Sachet, C. T. Shelton, Z. Liu, Z. Cheng, B.M. Foley, S. Graham, T. Luo, A. Henry, M.S. Goorsky, J. Shiomi, J.-P. Maria, P.E. Hopkins, Thermal boundary conductance across heteroepitaxial ZnO/GaN interfaces: assessment of the phonon gas model, Nano Lett. 18 (12) (2018) 7469–7477.
[38] L. Yang, B. Yang, B. Li, Enhancing interfacial thermal conductance of an amorphous interface by optimizing the interfacial mass distribution, Phys. Rev. B 108 (16) (2023): 165303.
[39] Z. Zong, S. Deng, Y. Qin, X. Wan, J. Zhan, D. Ma, N. Yang, Enhancing the interfacial thermal conductance of Si/PVDF by strengthening atomic couplings, Nanoscale 15 (40) (2023) 16472–16479.
[40] Q. Wang, X. Wang, X. Liu, J. Zhang, Interfacial engineering for the enhancement of interfacial thermal conductance in GaN/AlN heterostructure, J. Appl. Phys. 129 (23) (2021): 235102.
[41] M.P. Tosi, F.G. Fumi, Temperature dependence of the Debye temperatures for the thermodynamic functions of alkali halide crystals, Phys. Rev. 131 (4) (1963) 1458–1465.
[42] P.E. Hopkins, J.L. Kassebaum, P.M. Norris, Effects of electron scattering at metal-nonmetal interfaces on electron-phonon equilibration in gold films, J. Appl. Phys. 105 (2) (2009): 023710.
[43] T. Zeng, G. Chen, Nonequilibrium electron and phonon transport and energy conversion in heterostructures, Microelectron. J. 34 (3) (2003) 201–206.